сообщения
объединенного
института
ядерных
исследований
дубна

E13-91-474

L.M.Soroko

ACCEPTANCE OF THE FOURIER TRANSFORM MICROSCOPES FOR NUCLEAR EMULSION

1991

The empirical approaches of this kind with its trials and errors have some drawbacks. To overcome these shortages and to find the real criteria for objective comparison of the various designs and proposals some invariant factors of the merits have to be set into the basis of the more fundamental investigations. For this purpose a new term: "acceptance of the Fourier transform microscopes" for nuclear emulsion is introduced. It is shown that this term is of the universal feature and can be used in various designs of these microscopes. In the frame of this new approach the problem of the measurement of the dip angle of the straight line particle track by means of the FT microscopes is analysed. The structure of the signals at the output of the FT microscope in the real conditions is presented.

2. ACCEPTANCE OF THE FT AND MFTM

The acceptance of these microscopes, FT and MFTM, $d\Omega$, is defined in general case as a product of its spatial, $d\Omega_{\vec{x}}$, and its angular, $d\omega_{\vec{\theta}}$, parts:

$$d\Omega = d\Omega_{\vec{x}} \cdot d\omega_{\vec{\theta}}. \qquad (1)$$

In the case of the straight line particle track this new term represents the volume element of the 5-dimentional space which covers both the 3-dimentional spatial space $\vec{x}(x,y,z)$ and the 2-dimentional angular space $\vec{\theta}(\theta_{xy}, \theta_z)$, where θ_{xy} is the orientation angle and θ_z is the dip angle of the straight line particle track to be search for.

The spatial part of the acceptance is equal either to the volume of the illuminating region of the nuclear emulsion of the wide a, of the height h and of the length D or the corresponding volume of the observation zone with transversal dimension Δx, where Δx is the spatial resolution of the MFTM.

Let us consider first the case of the horizontal straight line particle track with no degrees of freedom along the dip angle θ_z. It is sufficient to estimate in this case the angular part of the acceptance $d\omega_\theta = d\theta_{xy}$ along the orientation angle θ_{xy}. If the width of the transmitting slit of the detected system[12], Δ, is equal to the effective width of the FT of the straight line particle track $\Delta\omega$, where

$$\Delta\omega = \frac{\lambda H}{D}, \qquad (2)$$

λ is the wavelength of the light and H is the distance from the nuclear emulsion layer to the FT plane $\vec{\omega}$ (ω_x, ω_y), the angular part of the acceptance of the detected system is equal to

$$d\omega_\theta = d\theta_{xy} = \frac{\Delta\omega}{R_0} = \frac{\lambda H}{DR_0}, \qquad (3)$$

where R_0 is the average distance from the transmitting slit to the optical axis of the FT microscope. The spacial part of the acceptance of the detected system is equal to

$$d\Omega_{\vec{x}} = a \cdot h \cdot D, \qquad (4)$$

and the total acceptance of the detected system,

$$d\Omega = d\Omega_{\vec{x}} \cdot d\theta_{xy} = ahD\,\frac{\lambda H}{DR_0} = \frac{a\lambda hH}{R_0}, \qquad (5)$$

does not depend on the length of the illuminating region D. For h = 200 μm, λ = 0.6 μm, H = 150 mm, R_0 = 80 mm and a=20 μm we have

$$d\Omega = \frac{20\cdot10^{-3}\cdot0.2\cdot0.6\cdot10^{-3}\cdot1.5\cdot10^{2}}{0.8\cdot10^{2}} = 4.5\cdot10^{-6}\ \text{mm}\cdot\text{rad}. \qquad (6)$$

Now let us consider the MFTM with one-channel photodetectors and with transmitting slit set up directly ahead of the meso-optical mirror with ring response. The spatial part of the acceptance for this device will be equal to

$$d\Omega^0_x = \frac{\lambda}{\sin\alpha_{1/2}} \cdot \frac{a}{tg\alpha_{1/2}} \cdot D, \qquad (7)$$

where $\alpha_{1/2}$ is the angle between the central ray of the diffracted light and the optical axis of the microscope. For $\alpha_{1/2}$ = = 4/15 rad we have

$$d\Omega^0_x = \frac{0.6\cdot10^{-3}}{0.264} \cdot \frac{a\cdot D}{0.274} = 8.3\cdot10^{-3}\cdot aD. \qquad (8)$$

The total acceptance of the detected system of the MFTM with one-channel photodetectors and with transmitting slit in the vicinity of the meso-optical mirror with ring response is equal to

$$d\Omega_t = d\Omega^0_x \cdot d\omega^0_\theta = 8.3\cdot10^{-3}\cdot \frac{a\lambda H}{R_0} = 1.86\cdot10^{-7}\ \text{mm}\cdot\text{rad}. \qquad (9)$$

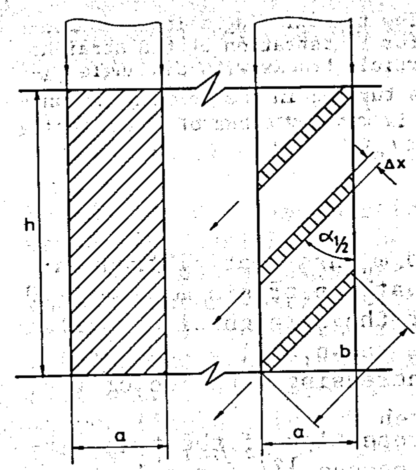

Fig.1. The illuminated region of the nuclear emulsion layer of the thickness h in the FT microscope of the direct observation (left) and the observation zone of the MFTM (right).

Both in the FT microscope of the direct observation and in the MFTM with transmitting slit the total acceptance does not depend on the length of the illuminating region D.

From eqs.(6) and (9) we see that the acceptance of the MFTM with one-channel photodetectors and with transmitting slit in the vicinity of the meso-optical mirror with ring response is 23 times smaller than in the FT microscope of the direct observation with the same transmitting slit.

To understand this difference let us consider the cross sections of the illuminating system of the FT microscope of the direct observation[12] and of the observation zone of the MFTM with one-channel photodetectors (fig.1). In the FT microscope of the direct observation the area of the illuminating region is equal to a·h. In the MFTM with one-channel photodetectors and with transmitting slit the area of the observation zone is equal to

$$b\cdot\Delta x = \frac{\lambda}{\sin\alpha_{1/2}} \cdot \frac{a}{tg\alpha_{1/2}}. \qquad (10)$$

Thus the spatial selectivity of the second device is

$$\kappa = \frac{h}{\lambda}\,\sin\alpha_{1/2}\cdot tg\alpha_{1/2} \qquad (11)$$

times higher than in the first device. From (11) we see that for the extreme case $\alpha_{1/2}$= 1 rad $\lambda = 0.6\cdot10^{-3}$ mm, h=100×10^{-3}mm this advantage will be equal to ≈ 670:1.

3. MEASUREMENT OF THE DIP ANGLE θ

As has been explained in[13] the contour of the FT of the straight line particle track with dip angle $\theta_z \neq 0$ assumes the form of the circle arc which crosses the origin 0 of the FT

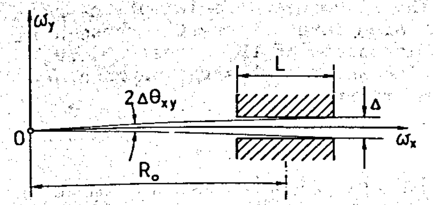

Fig.2. The transmitting slit in the position for registration of the straight line particle tracks with dip angle $\theta_z = 0$. The turning in the orientation angle θ_{xy} is made by means of the rotating folk /12/.

plane with $\omega_x = \omega_y = 0$, where ω_x and ω_y are spatial frequencies. The tangent to this circle arc at the origin $\omega_x = \omega_y = 0$ is perpendicular to the projection of the straight line particle track on the FT plane. As will be shown bellow the curvature of this circle arc, $1/\rho$, is the increasing function of the dip angle θ_z.

Let us consider the information properties of the transmitting slit in the FT plane of the microscope /12/ for selective detection of the particle tracks with given dip angle θ_z. The features of the system shown in Fig.2 are defined by the width of the transmitting slit Δ, by the length of the working part of the slit L and by the average distance R_0 from the central point of the working part of the slit to the optical axis of the microscope. In the position when the symmetry axis of the transmitting slit is oriented along the FT picture of the straight line particle track the system shown in Fig.2 sees effectively the straight line particle tracks with dip angle in the interval $\Delta\theta_z$ around $\theta_z = 0$.

There are two extreme cases. In the first one the slit width Δ is much more than the effective width of the FT of the straight line particle track, $\Delta\omega$, eq.(2). In the second case the slit width Δ is chosen equal to its optimal value

$$\Delta_{opt} = \frac{\Delta\omega}{2} = \frac{\lambda H}{2D} . \qquad (12)$$

Here we restrict ourselves to the first extreme case.

The transmitting slit in Fig.2 pickes up not only FT of the horizontal particle tracks with orientation angle $\theta_{xy} = 0$, but also FT of the particle

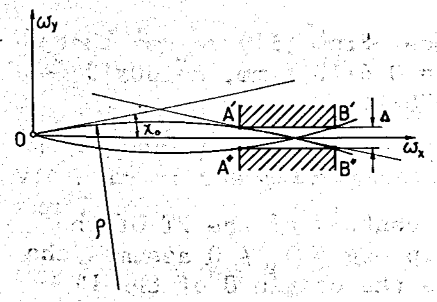

Fig.3. Two extreme positions of the FT pictures of the particle tracks with dip angles in the interval $\pm\Delta\theta_z$ picked up without any loss by the transmitting slit.

tracks with orientation angles in the interval $2\Delta\theta_{xy}$ around $\theta_{xy} = 0$, where

$$\Delta\theta_{xy} = \frac{\Delta}{2[R_0 + (\frac{L}{2})]} \approx \frac{\Delta}{2R_0} . \qquad (13)$$

Besides we see also particle tracks with dip angles in the interval $\Delta\theta_z$ which will be estimate below (Fig.3).

If the dip angle $\theta_z \gg \Delta\theta_z$, the fraction of the light of the FT picture picked up by the transmitting slit is getting small. To increase the transmitted light intensity we must introduce the eccentricity ε in the position of the transmitting slit with respect to the orientation of the (ω_x, ω_y) coordinate system (Fig.4). Let us determine the dependence between eccentricity ε, radius of the FT picture ρ and the angle θ_{xy}, at which the angular selectivity of the system will be shifted by this eccentricity. The angle χ_0 shown in Fig.3 defines the interval $\Delta\theta_z$ of the dip angles around $\theta_z^0 = 0$ for which the FT picture will be picked up completely by the transmitting slit in this new position.

The same results can be attained in the geometrical configuration shown in Fig.5 and produced as a result of two move-

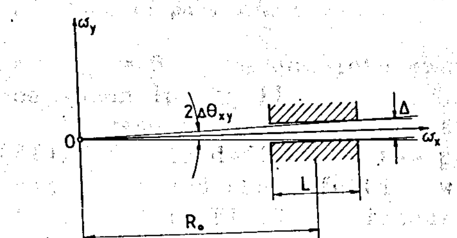

Fig.4. The transmitting slit in the position with eccentricity equal to ε. The turned angle θ_{xy} is changed in this position relative to the initial position without any eccentricity (upper).

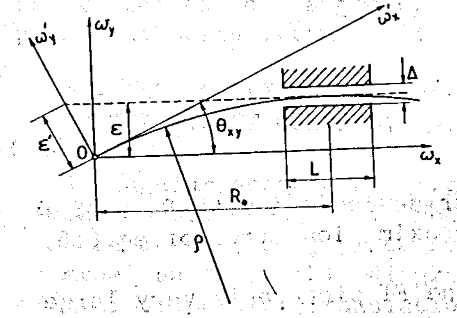

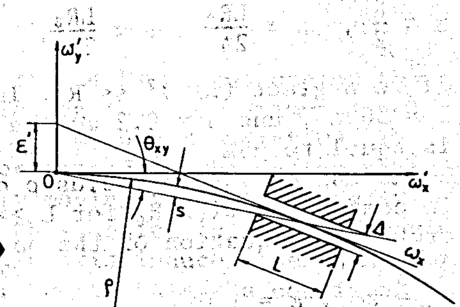

Fig.5. The position of the transmitting slit for registration of the particle tracks with dip angle $\theta_z > \Delta\theta_z$ after moving and rotation. In our approximation $\varepsilon \cong \varepsilon'$.

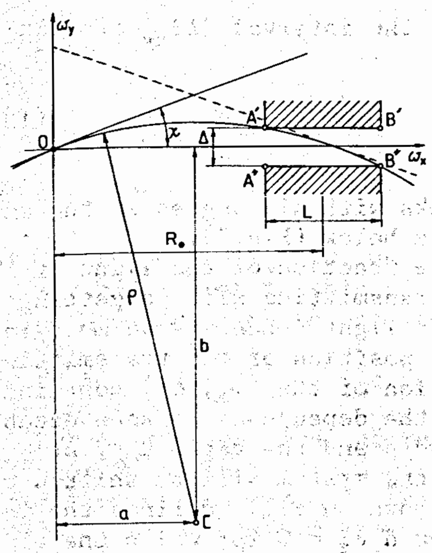

Fig.6. The circle arc OA′B″ of the FT picture in the extreme position for transmitting slit without eccentricity.

ments: shifting translationally and rotating of the transmitting slit. However, in practice it is easier to use the system with one movement. Therefore only system with translational movement of the transmitting slit will be treated here.

Let us determine the parameters of the circle which go through the origin 0 and the points A′ and B″ of the transmitting slit (Fig.6). The equation of this circle

$$(\omega_x - a)^2 + (\omega_y - b)^2 = \rho^2 \qquad (14)$$

has the following solutions:

$$a = \frac{R_0}{2}\left[1 + \left(\frac{L}{2R_0}\right)^2 + \left(\frac{\Delta}{2R_0}\right)^2\right],$$

$$-b = \frac{LR_0}{2\Delta}\left[1 - \left(\frac{L}{2R_0}\right)^2 - \left(\frac{\Delta}{2R_0}\right)^2\right], \qquad (15)$$

$$\rho = \frac{LR_0}{2\Delta}\left[1 - \left(\frac{L}{2R_0}\right)^2\right],$$

if we neglect $\Delta^4 \ll L^4$, and

$$a \approx \frac{R_0}{2}, \quad -b \approx \frac{LR_0}{2\Delta}, \quad \rho \approx \frac{LR_0}{2\Delta}, \qquad (16)$$

if we neglect $(L/2)^2 \ll R_0^2$. In our design[12] with $R_0 = 78$ mm, $L = 50$ mm, and $\Delta = 0.2$ mm the approximation error of eq.(16) is equal to ~3%.

As the curvature radius ρ of the FT picture is very large in comparison with R_0 for $L \gg \Delta$, we can present the circle arc by the equation of the parabola:

$$\omega_y = k\omega_x^2, \quad k = 1/2\rho. \qquad (17)$$

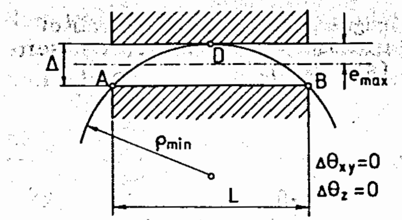

Fig.7. The circle arc ADB of the FT picture in the extreme position when $\Delta\theta_{xy} = \Delta\theta_z = 0$.

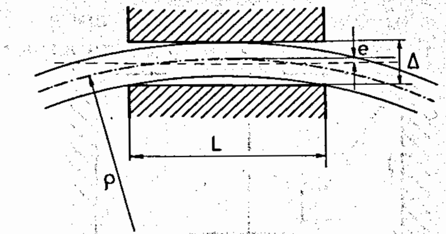

Fig.8. The FT pictures picked up effectively by the transmitting slit in general position with $e < \Delta/2$.

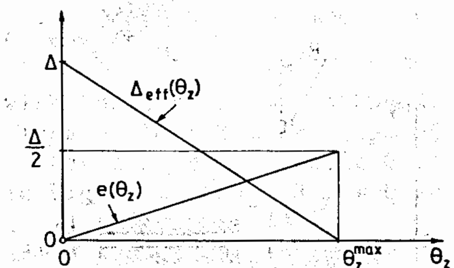

Fig.9. The depencies of effective width of the transmitting slit $\Delta_{eff}(\theta_z)$ and of parameter $e(\theta_z)$.

For $\omega_x = R_0$ we have

$$\omega_y\Big|_{\omega_x = R_0} = \xi \text{ and } \rho = \frac{R_0^2}{\Delta}. \qquad (18)$$

As we see from Fig.7 the detecting efficiency of the transmitting slit is equal to zero for $\rho = \rho_{min}$ in the configuration when the circle arc intersects the point A, D and B in Fig.7: $\Delta\theta_z = \Delta\theta_{xy} = 0$. More complete picture of this configuration will be shown in Fig.11.

In general case the detecting efficiency of the transmitting slit is defined by the parameter e shown in Fig.8. The parameter e and the effective width of the transmitting slit $\Delta_{eff}(\theta_z)$ in Fig.9 are linear functions of the dip angle θ_z: the bigger the dip angle θ_z the smaller the detecting efficiency of the transmitting slit.

4. ANGULAR ACCEPTANCE OF THE FT MICROSCOPE OF THE DIRECT OBSERVATION

An angular acceptance diagram of the FT microscope of the direct observation[12] is shown in Fig.10. The maximum angular acceptance is taking place for $\theta_{xy} = 0$, $\theta_z = 0$ (point 0). The external parts of this diagram correspond to the design of the FT microscope with translationally moving transmitting slit (see Fig.4). The main feature of this design is that the moving of the transmitting slit along ω_y - axis induces the change of the tuned orientation angle θ_{xy}. Due to this the centre of the acceptance in the form of the rectangular will be on the

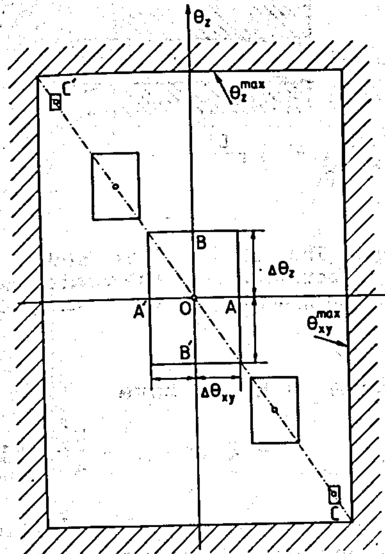

Fig.11. Complete geometry in the configuration with $\rho = \rho_{min}$ (see text).

Fig.10. Angular acceptance diagram of the FT microscope of the direct observation (see text).

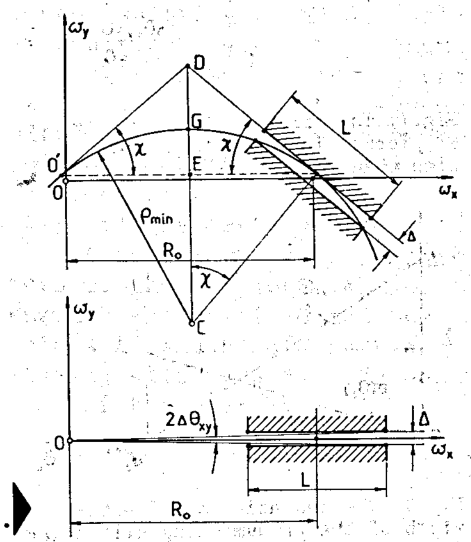

line CC′ (Fig.10). The points C and C′ present the extreme geometry shown in Fig.7 and Fig.11. In this configuration the radius curvature of the FT picture assumes its minimum value ρ_{min}. From Fig.7 we may estimate the parameters of this extreme circle arc with $\rho = \rho_{min}$. The equation of this circle arc in (ω''_x, ω''_y) coordinate system

$$(\omega''_x - \alpha)^2 + (\omega''_y - \beta)^2 = \rho^2_{min} \qquad (19)$$

has the following solution

$$\alpha = 0,$$
$$-\beta = \frac{L^2}{8\Delta}, \qquad (20)$$
$$\rho_{min} = \frac{L^2}{8\Delta}\left[1 + \left(\frac{2\Delta}{L}\right)^2\right].$$

The θ_{xy} - shift induced by the eccentricity of the transmitting slit will have in points C and C′ its maximum value

$$\theta^{max}_{xy} = \chi = \arcsin\frac{R_0}{2\rho_{min}} \approx \frac{4R_0\Delta}{L^2}. \qquad (21)$$

Now we must prove that the line CC′ goes throw the points D and D′ of the central acceptance rectangular for $\theta_{xy} = \theta_z = 0$ and thus

$$\frac{\Delta\theta_z}{\Delta\theta_{xy}} = \frac{\theta^{max}_z}{\theta^{max}_{xy}}. \qquad (22)$$

The dependence of the dip angle θ_z on the geometric parameter ξ defined by eq.(18) can be approximated for $\rho \gg R_0$ by the linear function

$$\theta_z = C_1 \cdot \xi_{max} \qquad (23)$$

with constant C_1 which has different values for different designs of the FT microscope of the direct observation.

For the central point 0 of the angular acceptance diagram in Fig.10 with $\theta_z = \theta_{xy} = 0$ we have $\xi = \Delta/2$ and

$$\Delta\theta_z = C_1 \cdot \frac{\Delta}{2}, \quad \Delta\theta_{xy} = \frac{\Delta}{2R_0}. \qquad (24)$$

For the points C and C′ of this diagram in Fig.10 we have

$$\theta^{max}_z = C_1 \cdot \xi_{max}, \quad \theta^{max}_{xy} = \chi_{max}, \qquad (25)$$

where

$$\xi_{max} = 2\overline{DE} = 4\Delta\left(\frac{R_0}{L}\right)^2 \text{ and} \qquad (26)$$
$$\chi_{max} = \frac{4R_0\Delta}{L^2}.$$

Thus we have

$$\frac{\theta^{max}_z}{\theta^{max}_{xy}} = \frac{C_1 \cdot 2\overline{DE} \cdot R_0}{2\overline{DE}} = C_1 \cdot R_0, \qquad (27)$$

and also

$$\frac{\Delta\theta_z}{\Delta\theta_{xy}} = \frac{C_1 \cdot \Delta \cdot 2R_0}{2\Delta} = C_1 \cdot R_0. \qquad (28)$$

The eq.(22) is proved.

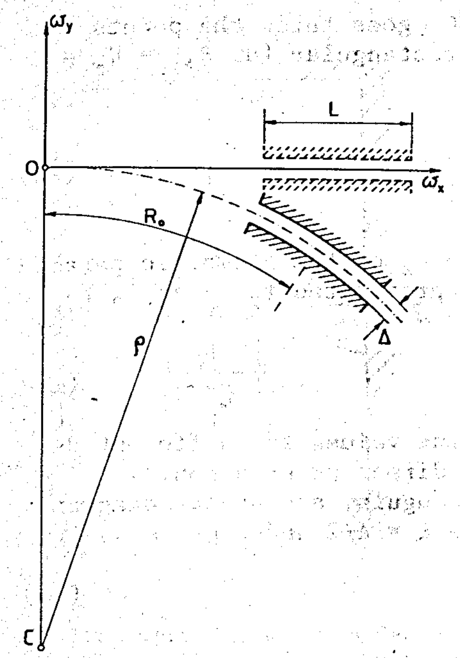

Fig.12. General view of the flexible transmitting slit of the constant clearence with bent degree of freedom for effective observation of particle tracks with any dip angle θ_z. The turning in the orientation angle θ_{xy} is made by means of the rotating folk[12].

For our design of the FT microscope[12]

$$C_1 = 2.82 \cdot mm^{-1} \cdot degree \quad (29)$$

and

$$\left.\begin{aligned} \Delta\theta_z &= 0.282° = 16.9' \\ \Delta\theta_{xy} &= 0.0735° = 4.4' \end{aligned}\right\} \quad (30)$$

$$\left.\begin{aligned} \theta_z^{max} &= 5.5°, \\ \theta_{xy}^{max} &= 1.43°. \end{aligned}\right\} \quad (31)$$

The best way to overcome the limit on the dip angle θ_z in our design is to use the flexible transmitting slit of the constant clearance and with bent degree of freedom (Fig.12).

5. STRUCTURE OF THE OUTPUT SIGNALS

To get some insight into the structure of the signals at the output of the FT microscope of the direct observation[12] we consider two kinds of the objects: a) particle tracks of very high linear density of silver grains, and 2) particle tracks of very small linear density of silver grains.

In the first case the intensity of the signal S from these particle tracks is much larger than the intensity of noise N induced by the randomly distributed silver grains, S >> N, and we can assume N = 0. After the multiplication of the signals from m photodetectors we get the product signal $Pr = S^m$ or $Pr = S^5$ in our case m = 5 if the particle track goes parallel to the symmetry axis of the transmitting slit (Fig.13). If the particle track has a dip angle $\theta_z \neq 0$, the FT picture of this particle track will form an angle α with symmetry axis of the slit. If $\alpha > \Delta/L$, the product signal Pr will be zero, as at least in one photodetector the signal will be zero.

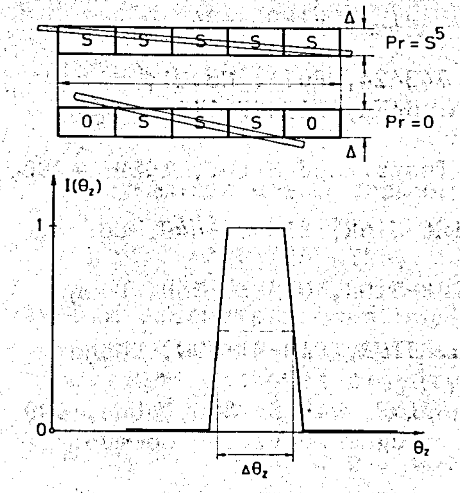

Fig.13. The structure of the product signal at the output of the FT microscope of the direct observation for the case of particle tracks of high ionization level.

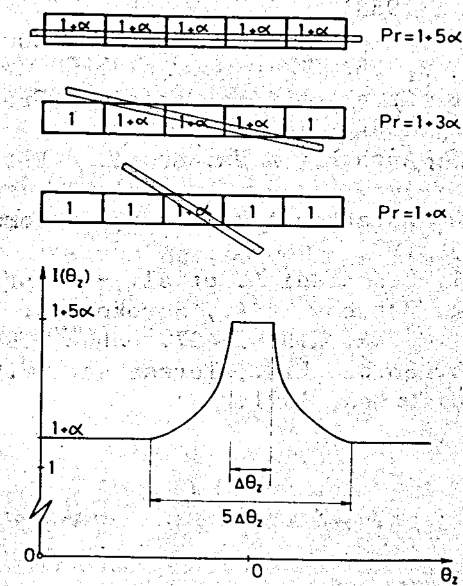

Fig.14. The structure of the product signal at the output of the FT microscope of the direct observation for the case of particle tracks of low ionization level.

In the second case the intensity of noise N will be larger than the intensity of the signal S: S << N. The normalized signal in every photodetector will be equal to $1 + \alpha$ with $\alpha = S/N << 1$. After the multiplication we get the product signal $Pr = (1 + \alpha)^k \approx 1 + \alpha k$, where k is the number of photodetectors illuminated by the FT picture. In the configuration of the transmitting slit without eccentricity the product signal will be ranged from $Pr^{max} = 1 + 5\alpha$ to $Pr^{min} = 1 + \alpha$ (Fig.14). Thus the total angular window $\Delta\theta_z$ will be equal to $5\,\Delta\theta_z^o$, eq.(30). In general case the response of the microscope versus dip angle θ_z will have an intermediate structure between the cases a) and b).

REFERENCES

1. Andreeva N.I. et al. - Commun.JINR, P1-85-692, Dubna,1985.
2. Vokal SD. et al. - Commun.JINR, P1-91-85, Dubna, 1985.
3. Batusov Yu.A. et al. - Preprint JINR, D1-88-932, Dubna, 1988.

4. Batusov Yu.A. et al. - Preprint JINR, E1-90-134, Dubna, 1990.
5. Soroko L.M. - USSR Patent No. 743424, Bull. No.21, p.262.
6. Astakhov A.Ya. et al. - Commun. JINR, P13-83-119, Dubna, 1983.
7. Astakhov A.Ya. et al. - Nucl. Instr. and Meth., 1989, A283, p.13.
8. Astakhov A.Ya. et al. - Preprint JINR, D13-89-449, Dubna, 1989.
9. Astakhov A.Ya. et al. - Preprint JINR, D13-89-450, Dubna, 1989.
10. Astakhov A.Ya. et al. - Commun. JINR, P13-91-299, Dubna, 1991.
11. Kisvaradi A. et al. - Preprint JINR, D13-89-550,Dubna,1989.
12. Batusov Yu.A., Soroko L.M., Terescghenko V.V. - Commun. JINR, E13-91-427, Dubna, 1991.
13. Soroko L.M., Tereschenko V.V. - Commun JINR, 13-91-204, Dubna, 1991.

Received by Publishing Department
on October 31, 1991.